National Weather Service
Office of Meteorology

Technical Procedures Bulletin

Subject: Changes to the NCEP Operational "Early" Eta Analysis / Forecast System

Series No. 447

Program and Plans Division, Silver Spring, MD 20910

ABSTRACT:

This Bulletin, written by Eric Rogers, Michael Baldwin, Thomas Black, Keith Brill, Fei Chen, Geoffrey DiMego, Joseph Gerrity, Geoffrey Manikin, Fedor Mesinger, Kenneth Mitchell, David Parrish, Qingyun Zhao of the NWS Environmental Modeling Center, National Centers for Environmental Prediction, describes changes to the Eta Forecast System which were approved at the December 2, 1997, CAFTI meeting.

Changes to the NCEP Operational "Early" Eta Analysis / Forecast System

**Eric Rogers, Michael Baldwin, Thomas Black, Keith Brill, Fei Chen,
Geoffrey DiMego, Joseph Gerrity, Geoffrey Manikin,
Fedor Mesinger, Kenneth Mitchell, David Parrish, Qingyun Zhao**

Environmental Modeling Center, National Centers for Environmental Prediction

1. INTRODUCTION

The National Centers for Environmental Prediction (NCEP) "Early" Eta analysis and forecasting system was operationally implemented in June 1993, replacing the Limited-Area Mesh Model in providing early forecast guidance over North America (Black et al., 1993, Rogers et al. 1995). The June 1993 system was comprised of 1) an Eta Regional Optimum Interpolation (OI, DiMego, 1988) analysis using a first guess from the NCEP Global Data Assimilation System (GDAS), and 2) a 48-h Eta model forecast at a resolution of 80-km with 38 vertical levels.

In 1995 two major improvements in mesoscale forecast guidance from NCEP were implemented. First, NCEP began twice-daily forecasts of a 29-km, 50 level eta model (Eta-29, Black, 1994) over the contiguous United States and adjacent areas in March 1995. A 33-h forecast from the Eta-29 is run from 0300 and 1500 UTC initial conditions after a 3-h spin-up cycle. Second, in October 1995 NCEP implemented the Eta-48 system to replace the 80-km Early Eta (Rogers et al., 1996) which included an increase in horizontal resolution to 48-km, and the use of the Eta Data Assimilation System (EDAS) to produce an analysis and first guess more consistent with the forecast model than that obtained from the GDAS. Model physics were enhanced in the 1995 upgrade with the introduction of a cloud prediction scheme (Zhao et al., 1997) and in January 1996 with a new land-surface model (Chen et al., 1996), a new viscous sublayer parameterization (Janjic 1996a) and a revised version of the Mellor-Yamada level 2.5 turbulence scheme (Janjic, 1996b). Examination of model surface temperature / moisture during 1996 showed that the skin temperature generally showed too large a diurnal cycle. Several factors contributed to this problem, including insufficient absorption of shortwave radiation, underestimates of cloud, and a negative bias in surface evaporation. To address these concerns several modifications to the model radiation package and land-surface model (Black et al., 1997, Betts et al., 1997) were implemented in the Eta-48 and Eta-29 systems in February 1997.

Recent studies (Baldwin and Black, 1996; Schneider et al. 1996; McDonald et al., 1998) have

the boundary than with the 48-km grid.

In order to partially alleviate any potential problem caused by a closer western boundary, two changes were made to the processing of the NCEP Aviation (AVN) model forecasts used as lateral boundary conditions. In the 48-km system, the EDAS / Early Eta computes boundary tendencies every 6-h from the **12-h old** AVN forecast. The Eta-29 computes boundary tendencies every 3-h from the **current** AVN forecast. In the Eta-32, boundary tendencies will be computed every 3-h from the previous AVN forecast. Since the AVN is now run every 6-h (Iredell and Caplan, 1997), tendencies computed from the "off-time" AVN (0600 and 1800 UTC start time) will be used for the last 6-h of the EDAS and for the 48-h forecast.

The vertical structure of the Eta-48 is shown in Fig. 2a , the Eta-29 in Fig. 2b , and the Eta-32 in Fig. 2c . As with the horizontal grid, the choice of 45 vertical layers represents a compromise between the 38 levels in the Eta-48 and the 50 levels in the Eta-29. In order to allow the Eta-32 to better resolve low-level mesoscale structures in mountainous areas (like the western United States and Alaska) most of the extra model levels were added below 700 mb.

An example in model terrain differences between the Eta-29, Eta-32, and Eta-48 model grids over northern California is shown in Fig. 3 . The Eta model uses step-mountain orography, in which after interpolation to the eta native grid (a semi-staggered Arakawa e-grid), the step-mountain is raised or lowered to the closest vertical interface. Since the 3 models depicted in Fig. 3 have a different vertical structure, the steps will not be at the same elevation in each model.

As expected, the Eta-29 and Eta-32 model orography shows considerably more detail than the the Eta-48, particularly in differentiating between the Sierra Nevada and Cascade ranges in northern California. One obvious difference between the Eta-29 and Eta-32 models is in the depiction of the Great Basin in northern Nevada. The Eta-29 terrain shows most of the region at one elevation, while in the Eta-32 this region is depicted on 3 different steps. This difference is due to a modification of the Eta model orography algorithm toward one that is more "valley-favoring" (Mesinger, 1997, personal communication) that adds more small-scale detail.

The impact of the increase in resolution to 32-km / 45 levels is seen in Table 1, which shows the observed elevation, and the terrain height in both the Eta-48 and Eta-32 at selected rawinsonde stations in the western United States. Of the 13 stations listed, 12 moved closer to the observed elevation. Although grid-cell mean terrain height, by definition, will continue to be higher than

Table 1 - The Impact of the Increase in Resolution

Station name	WMO Station ID	Observed Elevation (m)	Eta-48 terrain height (m)	Eta-32 terrain height (m)
Boise, ID	72681	874	1252	941
Great Falls, MT	72776	1130	1252	1194
Glasgow, MT	72768	700	845	708
Riverton, WY	72672	1703	1743	1665
Reno, NV	72489	1515	1743	1665
Mercury, NV	72387	1009	1487	1194
Elko, NV	72582	1608	2021	1839
Salt Lake City, UT	72572	1288	1743	1839
Grand Junction, CO	72476	1475	2321	2213
Denver, CO	72469	1625	2021	1665
Flagstaff, AZ	72376	2192	2021	2213
Tucson, AZ	72274	779	1252	1063
Albuquerque, NM	72365	1620	2021	1839

2.2 The regional 3-dimensional variational analysis

A regional 3DVAR analysis has been developed for use in the EDAS (Parrish et al., 1996) as a replacement for the Eta OI analysis system. It is patterned after the NCEP global spectral statistical interpolation analysis (Parrish and Derber, 1992) with several differences. First, the background error statistics are simulated in grid space instead of model space, using a recursive

"isolated" temperature observations, such as the high density ACARS temperature data. The 3DVAR analysis can also assimilate other data types (such as radial velocities from NEXRAD radars, and direct radiances from GOES or polar orbiting satellites) which are not easily adapted for use in the NCEP regional OI analysis.

From 1996 onward the 3DVAR analysis has undergone extensive parallel testing in an 80-km EDAS, with an 80-km Eta OI EDAS as control. Fig. 4 shows the RMS temperature error versus rawinsonde data of the OI and 3DVAR analyses at the end of the 12-h EDAS cycle (valid at 0000 and 1200 UTC) for October 1996. The 3DVAR analysis has lower RMS errors at most of the mandatory pressure levels. The greatest differences are seen above 250 mb, where one would expect the use of ACARS temperature data to have the greatest impact. A similar signal was seen in the RMS wind and specific humidity errors (not shown). RMS temperature errors for the 12-h through 48-h forecasts (not shown) had a similar signal, with the greatest impact from the 3DVAR analysis seen between 300 and 150 mb.

The equitable threat score (ETS) and bias score for 80-km Eta model forecasts from the OI and 3DVAR analyses for August - November 1996 are shown in Fig. 5 . These charts show that the 3DVAR has a small positive impact on precipitation forecasts at nearly all thresholds.

The 3DVAR will use all the data types that are used in the OI analysis :

- Rawinsonde mass and wind
- Pibal winds
- Dropwinsondes
- Wind profilers
- Surface land temperature and moisture
- Oceanic surface data (ships and buoys)
- Aircraft winds
- Satellite cloud-drift winds
- Oceanic TOVS thickness retrievals
- GOES and SSM/I precipitable water retrievals

With the operational implementation of the 3DVAR analysis in the Eta-32 system, the following additional data types will be used which were not analyzed by the OI analysis:

- ACARS temperature data

2.3 Continuously cycled EDAS / 4-layer soil model

The EDAS which runs as part of the Eta-48 system is a 12-h assimilation with 3-h analysis updates, initialized from the GDAS. Initial values of soil parameters are obtained from the GDAS. The latter has had significant soil moisture biases (Wu et al., 1997), owing to biases in the 6-h global model forecast of precipitation and solar insolation. Most notable is the GDAS positive soil moisture bias in the southeast United States during the warm season. In the Eta-48 and Eta-29 model codes, an arbitrary adjustment of the input GDAS soil moisture is applied at the beginning of the EDAS to mitigate the aforementioned bias.

EMC has developed the capability to run the EDAS in continuous cycling mode, in which the previous EDAS run is used to initialize the next cycle (Rogers et al., 1996). The option exists to run either "full" cycling, in which all variables (atmospheric winds/temperature/moisture plus soil moisture / temperature, cloud water, and turbulent kinetic energy (TKE)) are cycled, or "partial" cycling, in which the soil, cloud, and TKE parameters are cycled but the first guess atmospheric state variables are obtained from the GDAS.

Although experiments at 80-km resolution (Rogers et al., 1996) show no adverse impact from full cycling and minor positive impact on quantitative precipitation skill scores, NCEP has decided that with the multitude of changes described above, a more conservative approach to cycling would be prudent. Therefore, in this package of changes the EDAS has been modified to run in partial cycling mode. The soil moisture pattern which evolves from the continuous EDAS is used to initialize all Eta model forecasts. Since the EDAS/Eta model has lower precipitation biases than the GDAS (Mesinger, 1996), use of a cycled EDAS will lead to improved soil moisture. An improved depiction of soil moisture during the model integration leads to a better simulation of the surface processes (fluxes, evaporation, etc) with positive impact on 2-m temperature and humidity, boundary layer profiles, convective indices and precipitation. Further improvements are anticipated in future Early Eta upgrades when the cycled EDAS is modified to assimilate hourly precipitation (Lin et al., 1998) and cloud observations (Zhao et al., 1998).

As part of the Eta-32 the number of soil layers is increased from two to four. In the Eta-48 and Eta-29, the original choice of two layers and their thicknesses (top layer of 10 cm and bottom layer of 190 cm) was driven by the fact that the initial soil moisture for the 48-km EDAS was taken from the GDAS, which has the same soil layer configuration. The 190 cm bottom layer physically acted as a deep root zone for transpiration through the vegetation canopy. Experience with both the GDAS and EDAS (Betts et al., 1996; Betts et al., 1997) showed that this very deep

for the addition of the physics of frozen soil, which will be included in a future upgrade.

An example of the difference in the near-surface layer volumetric soil moisture between the 48-km and 32-km EDAS is shown in Fig. 6 . The soil moisture shown in the 32-km EDAS had been cycling for 2 weeks. The 32-km EDAS soil moisture shows more small scale structure than the 48-km, which is due to a) sharper precipitation gradients, b) more soil layers, and c) more spatially variable soil and vegetation types in the EDAS than the GDAS. Most noteworthy is the sharper soil "dry line" across Texas, Oklahoma, and Kansas in the cycled EDAS. Significant differences are seen over New England and Florida which are due to the retention of soil moisture in the 32-km system caused by EDAS precipitation during the 2 weeks of continuous cycling.

2.4 Eta Model Physics / Dynamics modifications

Two changes to the Eta model's physics / dynamics were made as part of this upgrade. The first concerns the computation of the master length scale which is needed for the vertical turbulence transport via the model's Mellor-Yamada scheme (Janjic, 1990). In the January 1996 upgrade to the Early and Meso Eta described in section 1, the master length scale is calculated at model interfaces. In the Eta-32 upgrade, this procedure has been changed so that the master length scale is computed at the mid-point of the model layers, and the interface value is computed by averaging the two nearest layer values. If one imagines eddies within a model layer to be of a characteristic size appropriate to the layer thickness, and if one accords each layer an equal role in the turbulent exchange between two layers, then averaging of the master length scales of two adjacent layers appears to be the more justified approach to the problem.

The second change involves a modification to the main driver that calls the primary subroutines in the Eta model code. The Eta model uses the split explicit approach of integration which means that the fundamental variables are updated with new tendencies after each major dynamical or physical process has been described. Previously, the order of events in the dynamics were as follows: (1) the mass field was updated by the continuity equation; (2) the mass and wind fields were updated by horizontal and vertical advection; (3) the winds were updated by inertial gravity wave adjustment. Steps 1 and 3 comprise the so-called adjustment process. In the new driver in the 32-km upgrade, step 3 immediately follows step 1 so that both the mass and wind fields are updated by the adjustment process before the advection step begins. This change removes fictitious gravity waves that occasionally appeared in the forecasts, as illustrated in the Eta-29 example given in Fig. 7a and Fig. 7b .

3.1 Objective Scores

3.1.1 Grid-to-Observation Verification - EDAS first guess

One measure of the relative performance of the Eta-32 EDAS is to measure the fit of the "on-time" first guess (used by the 3DVAR or OI analysis from which the 48-h forecast is run) at 0000 and 1200 UTC. The height (500 and 250 mb, Fig. 8a), temperature (850 and 250 mb, Fig. 8b), and vector wind (950 and 250 mb, Fig. 8c) RMS errors against all observations for the Eta-48 EDAS and Eta-32 EDAS are shown in Fig. 8 for the period 27 October - 23 November 1997. The lower and middle tropospheric errors in the Eta-32 EDAS are consistently smaller for the entire period, indicating that the Eta-32 EDAS with the 3DVAR analysis provides a better first guess to the on-time analysis than the Eta-48 EDAS with the OI analysis. The Eta-32 250 mb wind errors tend to be lower than the Eta-48 for most cycles but the differences between the two are smaller than seen at 950 mb. The 250 mb height RMS error traces show no clear signal, with a nearly 50-50 split between the Eta-32 and Eta-48. It is not clear why the signal seen at 500 mb is not repeated at 250 mb; a closer examination of the daily numbers (not shown) did not reveal any diurnal signal. Additionally, comparisons between concurrent 80-km OI and 3DVAR cycled EDAS parallel runs show a similar pattern (not shown), indicating that both resolution difference and continuous cycling are not the cause of the observed error patterns at 250 mb. The only source of upper tropospheric mass data over the U.S. at asynoptic times is the high-density ACARS temperature observations. Therefore, it is possible that by only having aircraft temperature data available for the off-time analyses in the 3DVAR EDAS, one could have a worse fit to the 250 mb **height** data (which consists solely of rawinsondes) at 0000 and 1200 UTC than in an OI EDAS which did not use aircraft temperature data.

3.1.2 Precipitation

The ETS and bias score of 24-h accumulated precipitation over the contiguous United States for the operational Eta-48 and the Eta-32 are depicted in Fig. 9 for the period 29 October - 24 November 1997. A total of 35 cases were used in this sample. At the highest thresholds above 1 inch the Eta-32 forecasts are more skillful, while at the lowest thresholds the Eta-48 forecasts are better. The bias scores indicate that the lower ETS at the rain-no rain threshold for the Eta-32 is due to overprediction of light rain amounts (which is obvious from a subjective evaluation of daily forecasts). Since the bias scores for the Eta-32 at the high thresholds are lower than the Eta-48 bias scores, the superiority of the Eta-32 forecast at these thresholds (based on the equitable threat score) is due not to overprediction but to an improved forecast of these heavy rain events by the Eta-32.

forecast it is closer to observations. The hourly trace of 2-m temperature for the 3-h through 48-h shows that the Eta-32 reduces the error seen in the Eta-48 temperature trace, with a significant reduction in the root-mean-square error (0.59 deg K for the Eta-32 versus 1.08 deg K for the Eta-48). This trend is reversed in the 2-m specific humidity trace, in which the average value from the Eta-32 is roughly 0.2 g/kg higher at most forecast hours. The average 10-m vector wind RMS error in the Eta-32 is slightly lower then the Eta-48 throughout the forecast, in spite of the 12% reduction in this error at 00-h, probably due to the 3DVAR analysis used in the Eta-32 system, which uses surface winds over land.

It is not clear why the Eta-32 has a worse fit to the 2-m moisture data and to the initial 2-m temperature data, given the improved fit to lower and upper tropospheric temperatures in the Eta-32 EDAS shown in Fig. 8b . It is possible that the treatment of surface temperature and moisture data in the 3DVAR analysis needs some refinement.

3.2 Two Case Studies

3.2.1 16-17 November 1997 : California Rains

Fig. 11 shows the 24-h observed precipitation across Northern California valid at 1200 UTC 17 November 1997. The precipitation data were obtained from the Office of Hydrology River Forecast Center rain gauge database. The precipitation is associated with a frontal boundary which moved onshore into Northern California around 1200 UTC 16 November and moved northward into Oregon and Washington during the next 12-24 hours. There is considerable variation in precipitation amounts reflecting orographic influences. One maximum is seen along the coast, undoubtedly the result of upslope flow caused by the Coastal Range with amounts as high as 94 mm / 24 h along the coast near 40N, 124W. The precipitation minimum inland in the Sacramento River valley is probably caused by downslope conditions. A second maximum is observed further inland, reflecting upslope flow caused by the Sierra Nevada Range (highest amounts around 40 mm observed northwest of Lake Tahoe (39N, 120W)) and the Cascade Range, with many stations around Shasta Lake (near 41N, 122W) reporting over 40 mm / 24 h.

Fig. 12 shows the 0-24 h forecast of accumulated precipitation from the Eta-29, Eta-32, and the Eta-48 valid at 1200 UTC 17 November 1997. Although none of the three models were able to predict the extreme amounts observed, there are significant differences between them. The Eta-48 model predicted the highest amounts (> 36 mm) north of Cape Mendocino (located at 40.5N 124.5W in Fig. 11), which appears to be an overprediction based on the observed precipitation seen north of 40N in Fig. 11. Both the Eta-29 and the Eta-32 predicted more

predicting lower precipitation amounts between the Coastal and inland ranges. Although Eta-32 did not make a perfect forecast, it is clear that is has the ability to predict orographically-driven mesoscale structure in the precipitation field as well as the Eta-29.

3.2.2 20 November 1997 : Oceanic Cyclogenesis

Fig. 13 shows the NCEP GDAS analysis of sea level pressure valid at 0000 UTC 20 November 1997 with surface observations of wind and sea level pressure. The frontal wave with central pressure of ~1010 mb at 0000 UTC 20 November deepened into a mature cyclone with a central pressure below 1000 mb by 1200 UTC 20 November (not shown) as it tracked northeastward towards the Canadian Maritimes. This deepening was in response to a strong 500 mb short-wave trough (not shown) which caused 12-h height falls of 80-140 m across eastern New England and Nova Scotia.

Fig. 14 shows the 48-h forecasts of sea level pressure from the Eta-48 (ETA) and the Eta-32 upgrade (PARA32) valid at 0000 UTC 20 November 1997, while Fig. 15 shows the 24-h forecasts from these two models valid at 0000 UTC 20 November 1997. These charts reveal that for two successive forecast cycles the operational 48-km Eta model was 12-h too fast in predicting the rapid deepening, as well as predicting development closer to the U.S. coast then was observed.

Given the many changes associated with the Eta-32 upgrade, it is not clear based on the above charts alone which component is responsible for this improved cyclone forecast. Concurrently with the Eta-32 parallel, EMC is running two 80-km EDAS parallel runs with the 3DVAR and OI analyses, which are identical to the 32-km system (partial cycling, 4-layer soil model) except for the use of the Eta OI analysis in one of the parallels. When the forecasts from these 80-km runs were examined (not shown), the 80-km 3DVAR parallel did better than the 80-km OI parallel. Thus, it appears that the use of the 3DVAR analysis is the reason the Eta-32 system produced a better forecast of this case of oceanic cyclogenesis then the Eta-48.

4. CONCLUSIONS AND FUTURE PLANS

This implementation will see no changes made to any of the products created from the Early Eta forecast suite which are available via facsimile and AFOS. Existing Early Eta products on the NWS Office of Systems Operations (OSO) server (IP address = 140.90.6.103, or on the World Wide Web at *http://www.nws.noaa.gov/oso/ftpgate.shtml*) and the NCEP anonymous ftp server (*nic.fb4.noaa.gov*) will not change. Since the Eta-32 system will eventually replace the Eta-29

conformal grid but with 1/6th the resolution (AWIPS grid #222, 188-km resolution with ~ 3000 grid points). Current users of grid #104 (90-km polar stereographic over North America) who use this grid because it covers the computational grid of the Eta-48 are encouraged to move towards using either of these new Lambert conformal grids. Initially the new Lambert conformal grid will be accessible on the NCEP side of the OSO server.

This initial implementation of the Eta-32 is intended to replace the Eta-48 EDAS and 48-h forecast from 0000 UTC and 1200 UTC initial conditions. The 0300 / 1500 UTC Eta-29 system will still run using the system described by Black (1994). Within 6-9 months after this implementation NCEP intends to make two further changes to the Eta forecast suite:

- Include off-time Eta-32 forecasts (initially out to 18-h) from 0600 UTC and 1800 UTC initial conditions. When the off-time Eta-32 forecasts are in place the 0300 and 1500 UTC runs of the Eta-29 will be turned off
- Modify the Eta model convective parameterization scheme to better predict convective precipitation, especially in mountainous regions like the western United States, and along the Gulf of Mexico and southeast Atlantic coastal area

5. REFERENCES

Baldwin, M. E., and T. L. Black, 1996: Precipitation forecasting experiments in the western U.S. with NCEP's mesoscale Eta model. Preprints, 11th AMS Conference on Numerical Weather Prediction, Norfolk, VA, 19-23 August 1996.

Betts, A. K., S. -Y. Hong, and H. L. Pan, 1996: Comparison of NCEP/NCAR reanalysis with 1987 FIFE data. *Mon. Wea. Rev.*, **124**, 1480-1498.

-------, F. Chen, K. E. Mitchell, and Z. I. Janjic, 1997: Assessment of the land surface and boundary layer models in two operational versions of the NCEP Eta model using FIFE data. *Mon. Wea. Rev*., **125**, 2896-2961.

Black, T. L., 1994: The new NMC mesoscale Eta model : Description and forecast examples. *Wea. Forecasting*, **9**, 265-278.

-------, D. G. Deaven, and G. J. DiMego, 1993: The step-mountain eta-coordinate model : 80-km "early" version and objective verifications. NWS Technical Procedures Bulletin 412, NOAA/NWS, 31 pp. [Available from National Weather Service, Office of Meteorology, 1325 East-West Highway, Silver Spring, MD 20910]

-------, and coauthors, 1997 : Changes to the Eta forecast systems. NWS Technical Procedures Bulletin 421, NOAA/NWS, 31 pp. [Available from National Weather Service, Office of Meteorology, 1325 East-West Highway, Silver Spring, MD 20910]

Chen, F. and coauthors, 1996 : Modeling of land-surface evaporation by four schemes and comparison with FIFE results. *J. Geophys. Res.*, **101**, 7251-7268.

DiMego, G. J., 1988 : The National Meteorological Center Regional Analysis System. *Mon. Wea. Rev.*, **116**, 977-1000.

Hayden, C. M., and R. J. Purser, 1995: Recursive filter objective analysis of meteorological field: applications to NESDIS operational processing. *J. Appl. Met.*, **34**, 3-15.

-------, 1996a : The surface parameterization in the NCEP Eta model. *Research Activities in Atmospheric and Oceanic Modelling*. CAS/JSC Working Group on Numerical Experimentation, WMO, 440 pp. [Available from WMO, CP No. 2300, CH-1211, Geneva 2, Switzerland]

-------, 1996b : The Mellor-Yamada level 2.5 turbulence closure scheme in the NCEP Eta model. Preprints, 11th AMS Conference on Numerical Weather Prediction, Norfolk, VA, 19-23 August 1996.

Lin, Y., K. E. Mitchell, E. Rogers, and M. E. Baldwin, 1998: Assimilation of real-time multi-sensor hourly precipitation observations into the NCEP Eta model. Preprints, 12th AMS Conference on Numerical Weather Prediction, Phoenix, AZ, 12-16 January 1998.
McDonald, B. E., J. D. Horel, J. Stiff, and W. J. Steenburgh, 1998: Observations and simulations of three downslope wind events over the northern Wasatch mountains. Preprints, 12th AMS Conference on Numerical Weather Prediction, Phoenix, AZ, 12-16 January 1998.

Mesinger, F., 1996 : Improvements in quantitative precipitation forecasts with the Eta regional and mesoscale models at the National Centers for Environmental Prediction. Preprints, 11th AMS Conference on Numerical Weather Prediction, Norfolk, VA, 19-23 August 1996.

Parrish, D. F., and J. Derber, 1992: The National Meteorological Center's spectral statistical interpolation analysis system. *Mon. Wea. Rev.*, **120**, 1747-1763.

-------, J. Purser, E. Rogers, and Y. Lin, 1996 : The regional 3d-variational analysis for the Eta model. Preprints, 11th AMS Conference on Numerical Weather Prediction, Norfolk, VA, 19-23 August 1996.

Rogers, E., D. G. Deaven, and G. J. DiMego, 1995: The regional analysis system for the operational Eta model : Original 80-km configuration and future changes. *Wea. Forecasting*, **10**, 810-825.

-------, T. L. Black, D. G. Deaven, G. J. DiMego, Q. Zhao, M. Baldwin, N. W. Junker, and Y. Lin, 1996 : Changes to the operational "early" eta analysis / forecast system at the National Centers for Environmental Prediction. *Wea. Forecasting*, **11**, 391-413.

-------, D. Parrish, Y. Lin, G. DiMego, 1996 : The NCEP Eta Data Assimilation System : Tests with a regional 3-d variational analysis and continuous cycling. Preprints, 11th AMS

Center. Preprints, 11th AMS Conference on Numerical Weather Prediction, Norfolk, VA, 19-23 August 1996.

Wu, W.-S., M. Iredell, S. Saha, and P. Caplan, 1997 : Changes to the 1997 NCEP operational MRF model analysis/forecast system. NWS Technical Procedures Bulletin 443, NOAA/NWS, 31 pp. [Available from National Weather Service, Office of Meteorology, 1325 East-West Highway, Silver Spring, MD 20910]

Zhao, Q., T. L. Black, and M. E. Baldwin, 1997 : Implementation of the cloud prediction scheme in the Eta model at NCEP. *Wea. Forecasting*, **12**, 697-712.

-------, and coauthors, 1998 : Assimilating cloud and precipitation observations in the Eta model to improve cloud and precipitation forecasts. Preprints, 12th AMS Conference on Numerical Weather Prediction, Phoenix, AZ, 12-16 January 1998.

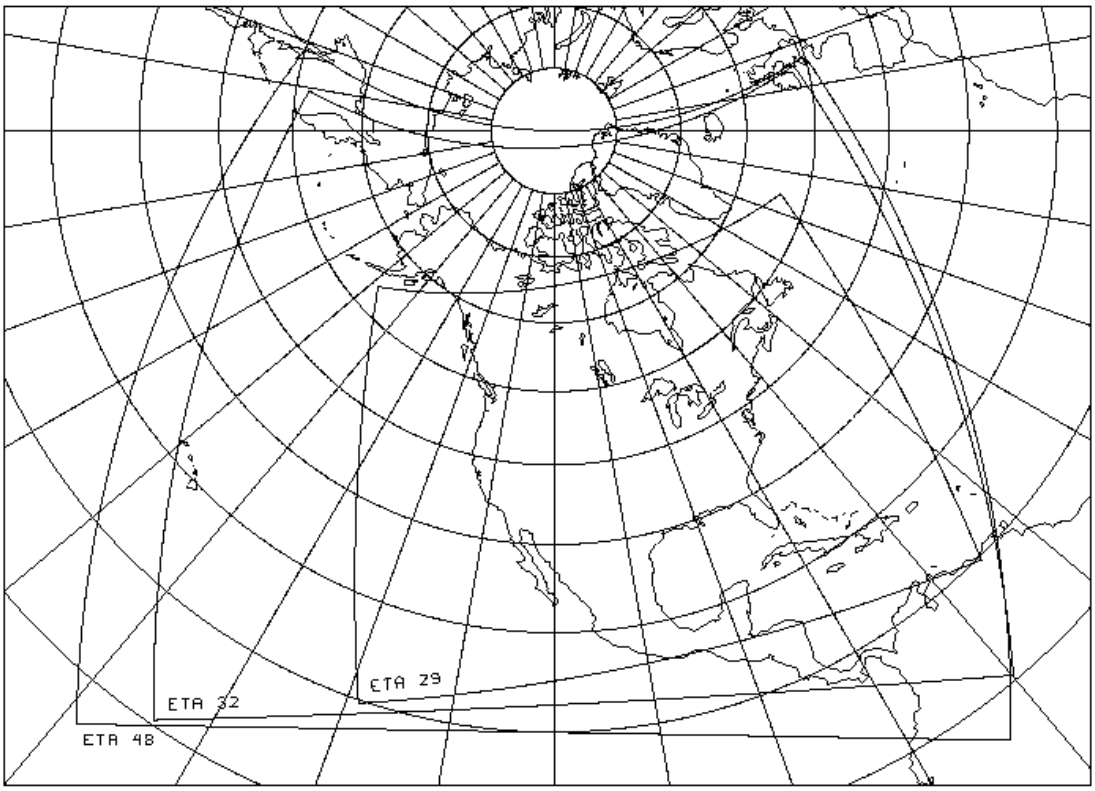

Figure 1: Horizontal domains of the Eta-48, Eta-29, and Eta-32.

Eta Model 38 – Layer Distribution

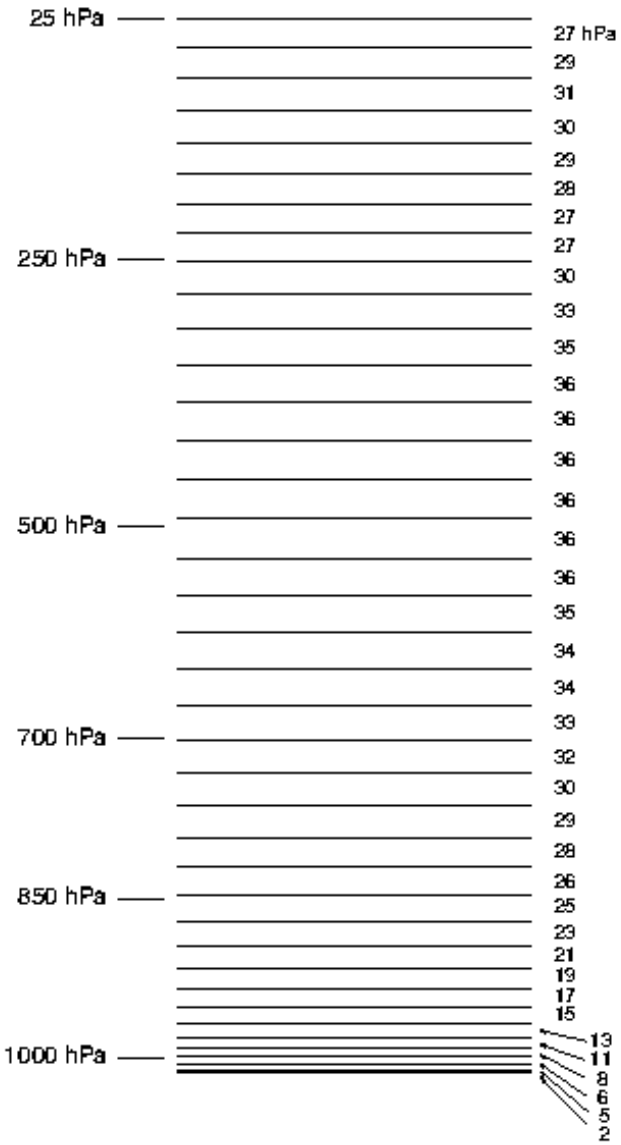

Figure 2: (a) The distribution of the 38 layers in the Eta-48. The pressure on the left side indicates the layers' position with respect to the standard atmosphere, while the number on the right give an approximate pressure depth of each layer.

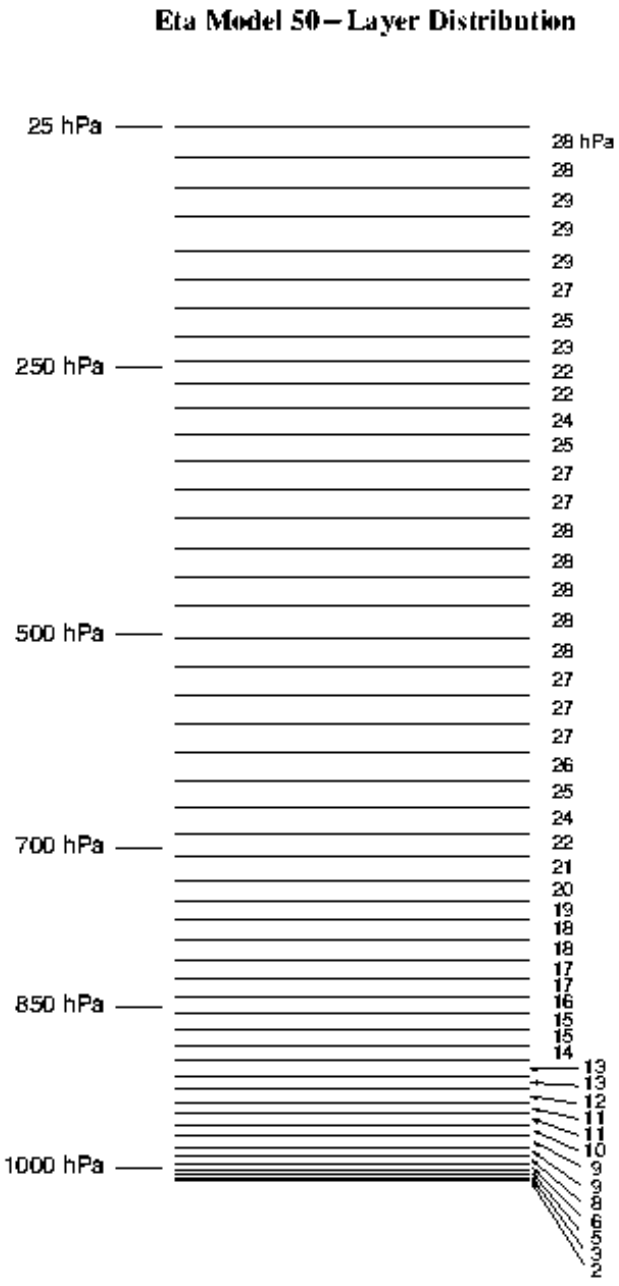

Figure 2: (b) Same as (a) but for the 50 layers of the Eta-29.

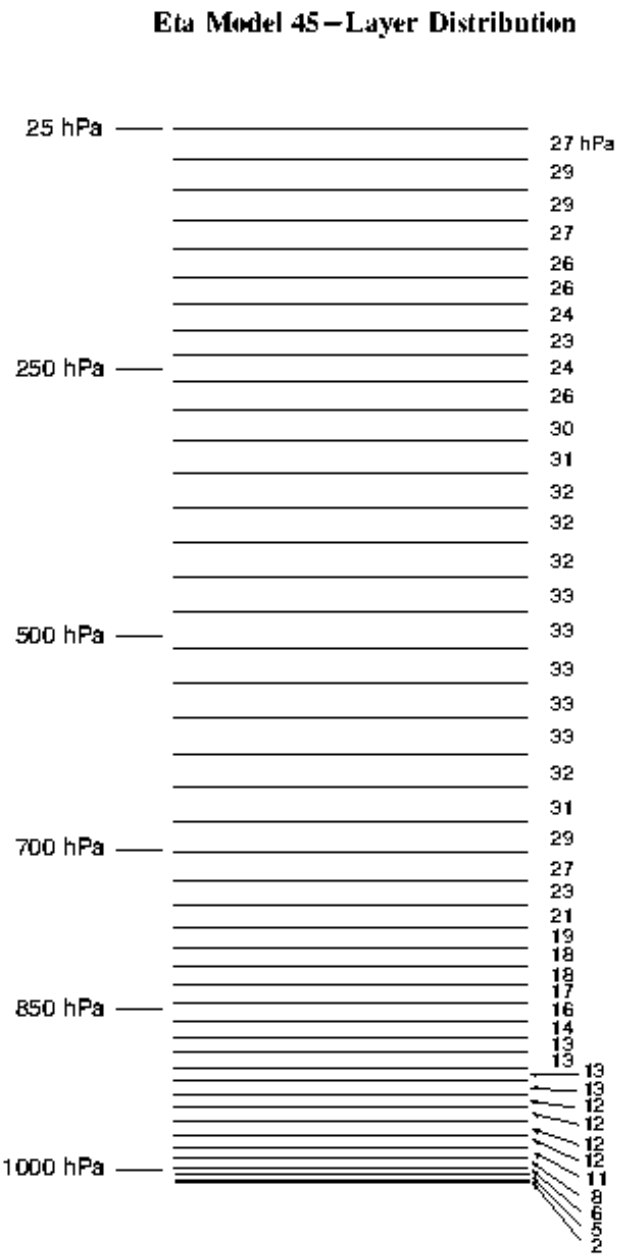

Figure 2: c) Same as (a) but for the 45 layers of the Eta-32 model.

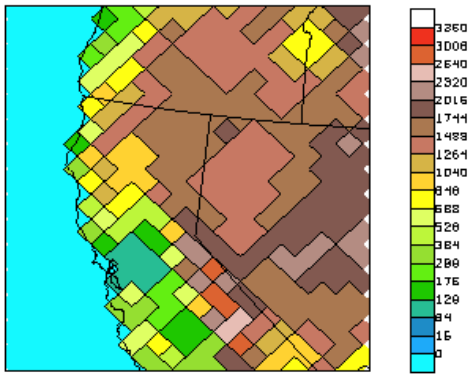

48-KM ETA TERRAIN

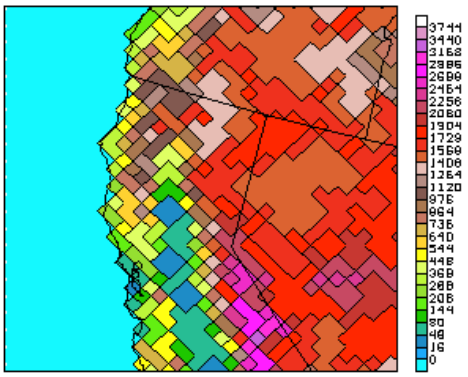

29-KM ETA TERRAIN

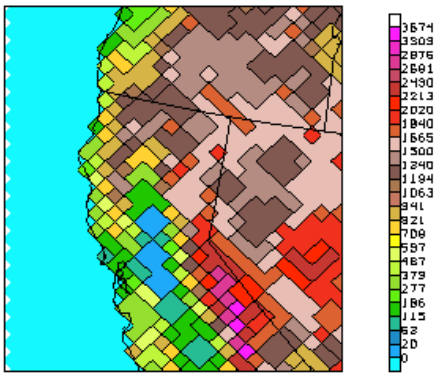

32-KM ETA TERRAIN

Figure 3: Eta model terrain height (m) over northern California for the Eta-48 (top), Eta-29 (bottom left), and the Eta-32 (bottom right).

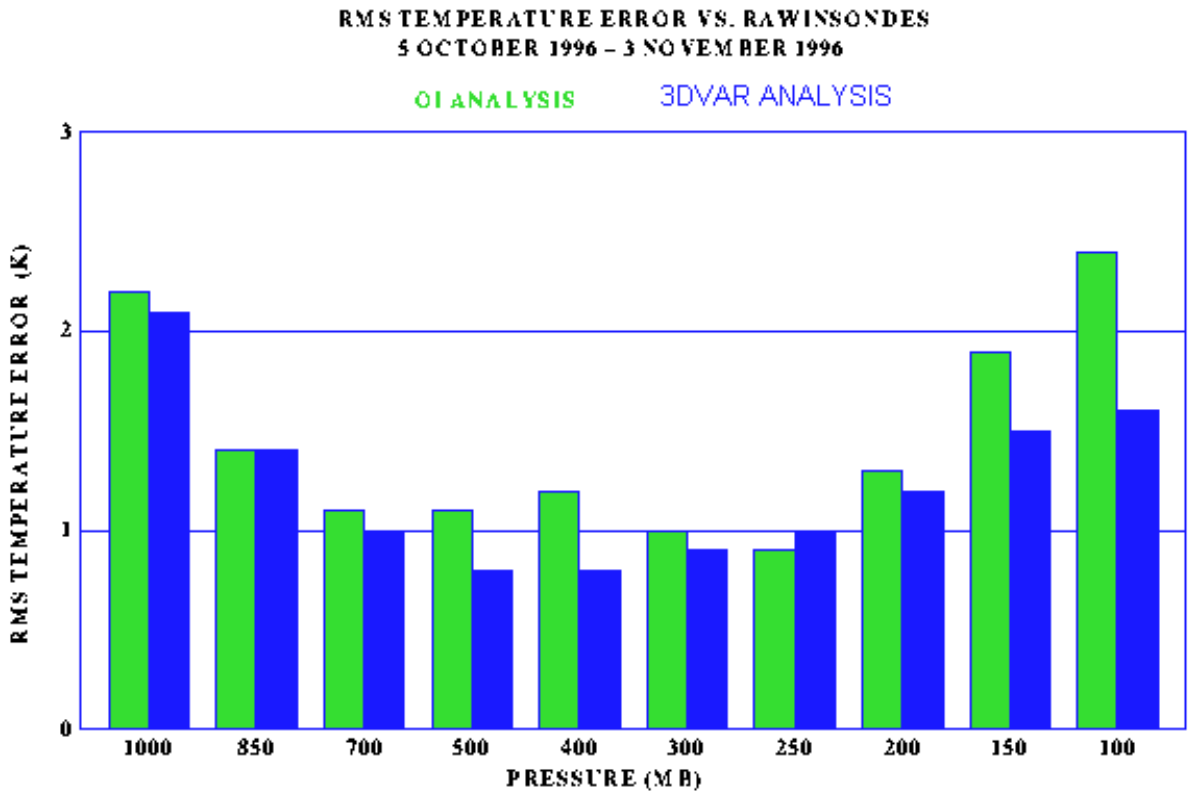

Figure 4. Root-mean-square temperature error (K) of the 80-km OI analysis (light bar) and the 80-km 3DVAR analysis (dark bar) versus rawinsonde data over the contiguous United States for 5 October - 3 November 1996.

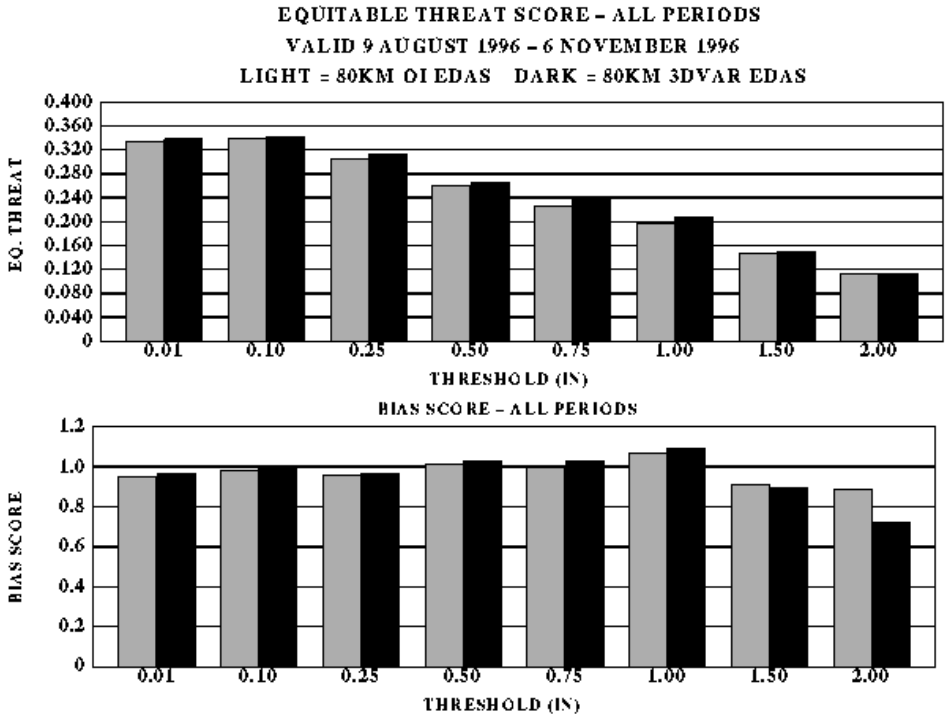

Figure 5. Equitable threat and bias scores for 24-h forecast accumulated precipitation from the 80-km Eta OI system (light bar) and the 80-km Eta 3DVAR system (dark bar) for all forecasts periods from 9 August 1996 - 6 November 1996.

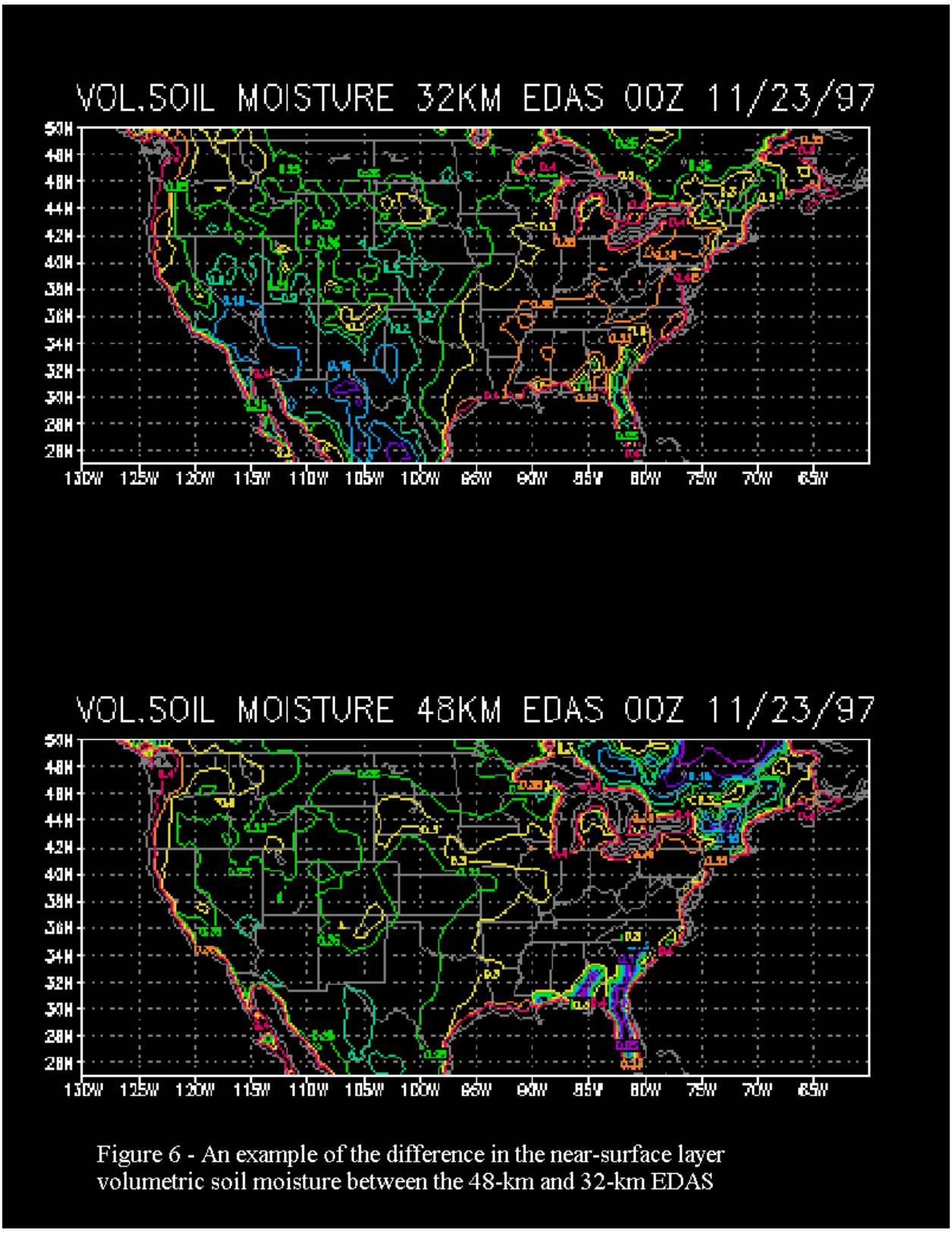

Figure 6 - An example of the difference in the near-surface layer volumetric soil moisture between the 48-km and 32-km EDAS

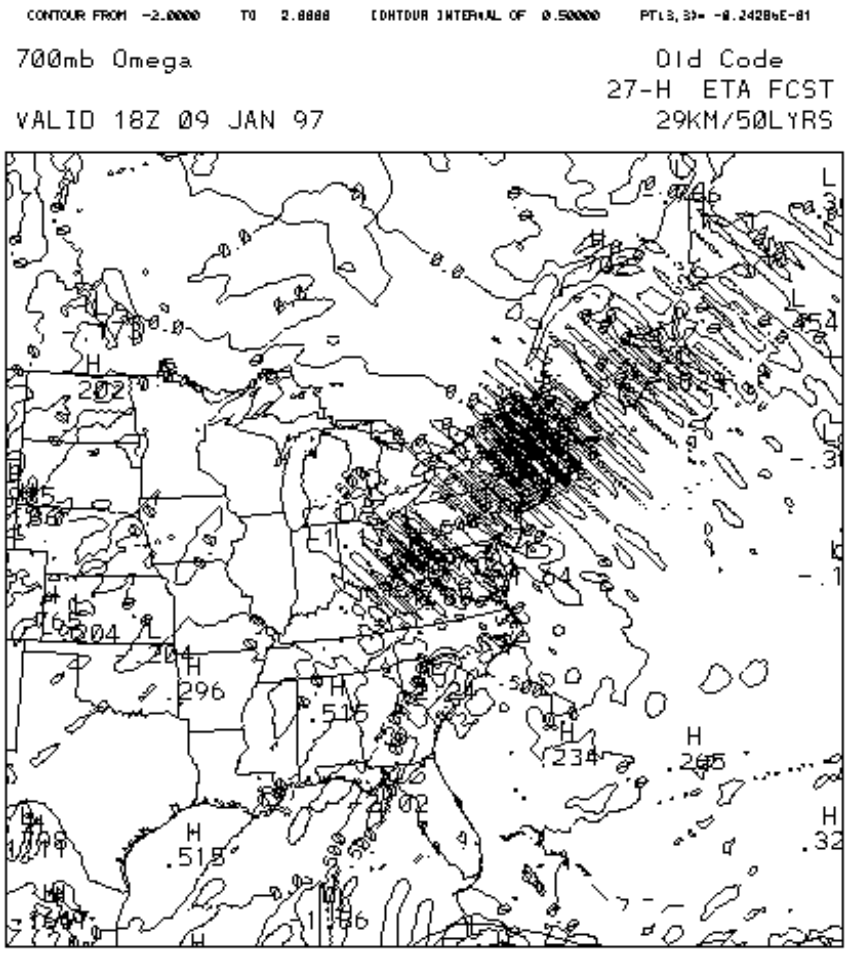

Figure 7. (a) 27-h forecast of 700 mb pressure vertical velocity (10-3 mb/s) from the operational Eta-29 forecast valid at 1800 UTC 9 January 1997.

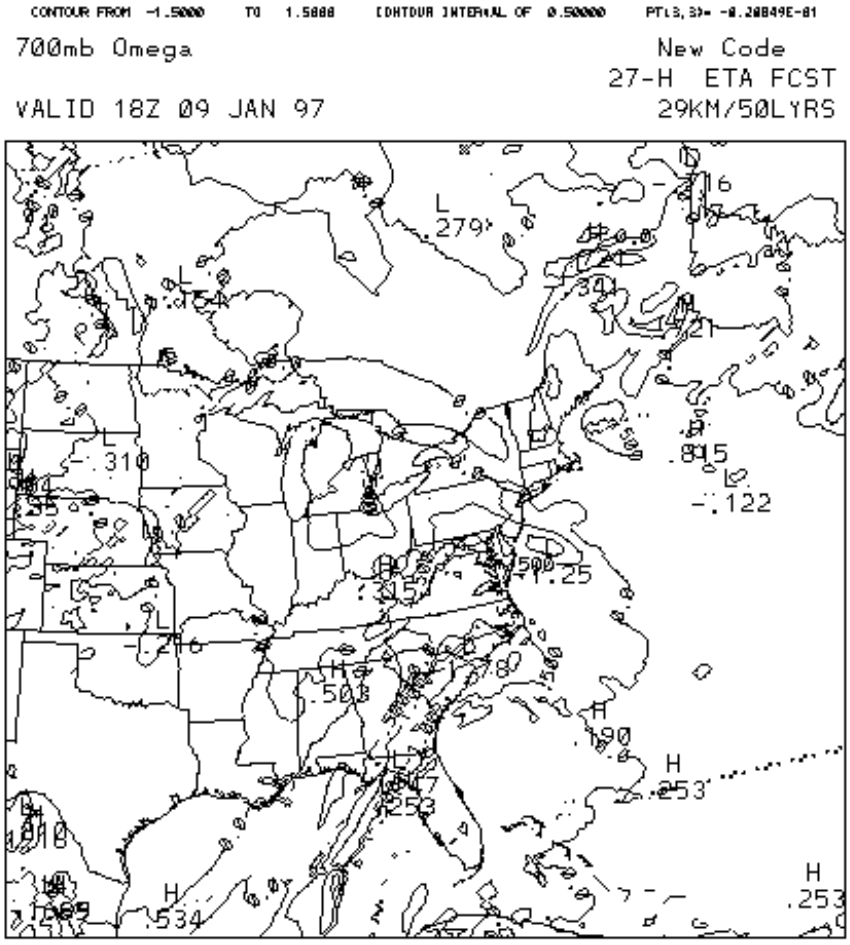

Figure 7 (b) Same as (a) but for a rerun of the Eta-29 forecast with the new model code. Contour interval = 0.5 x 10-3 mb/s.

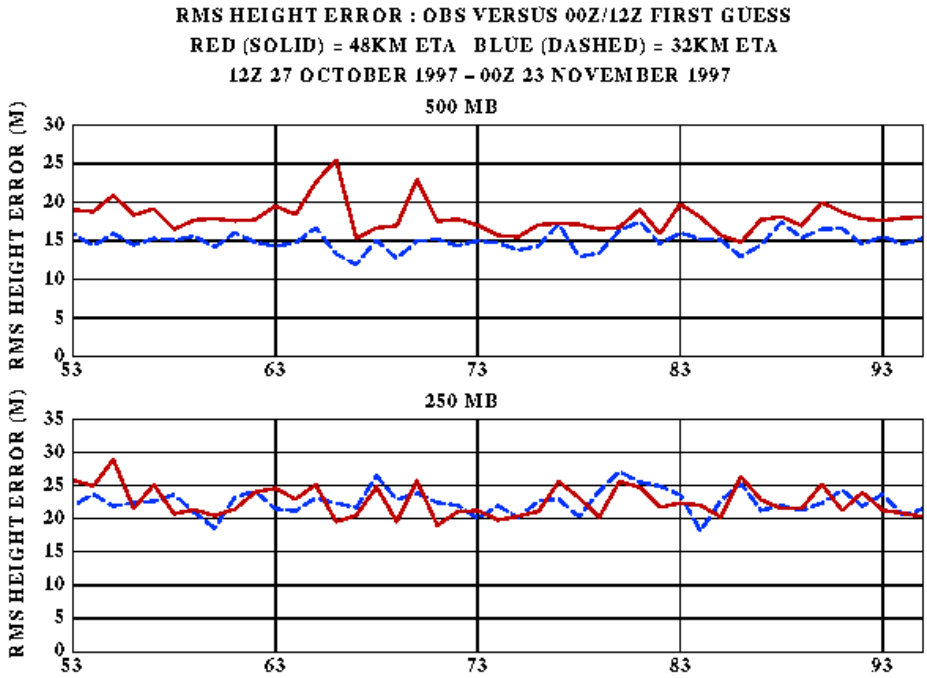

Figure 8. (a) Root-mean square error (against all observations) of the 500 and 250 mb geopotential height from the EDAS first guess valid at 0000 / 1200 UTC for the Eta-48 (solid red line) and the Eta-32 (dashed blue line) for the period 1200 UTC 27 October - 0000 UTC 23 November 1997. Number on the abscissa are cycles (53=1200 UTC 27 October 1997).

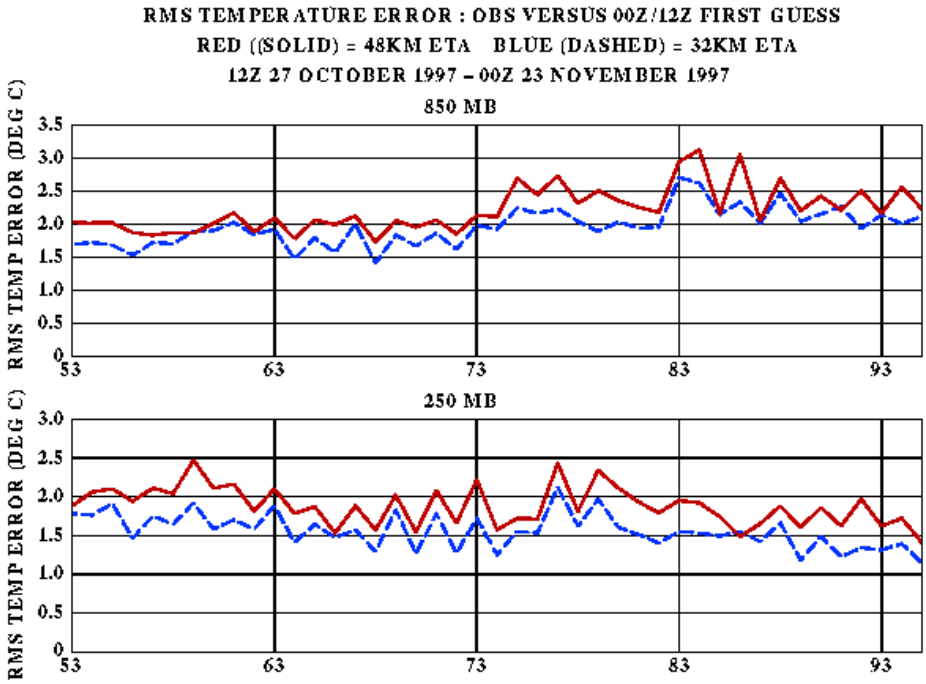

Figure 8. (b) Same as (a) but for 850 and 250 mb temperatures

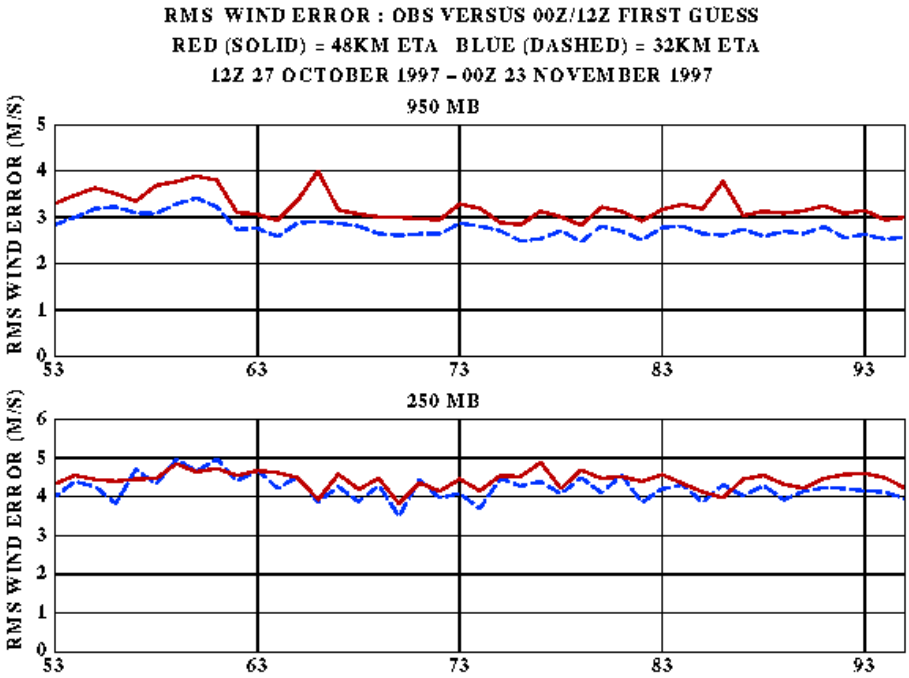

Figure 8. c) Same as (a) but for 950 and 250 mb vector wind.

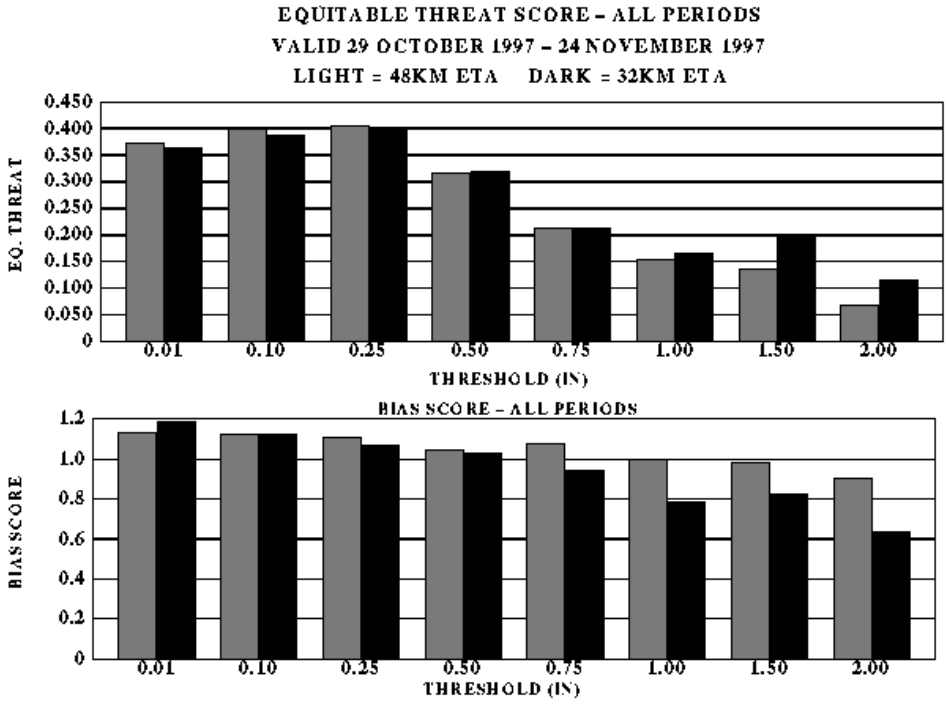

Figure 9. Same as Fig. 5 but for the Eta-48 (light bar) and the Eta-32 for the period 29 October 1997 - 24 November 1997.

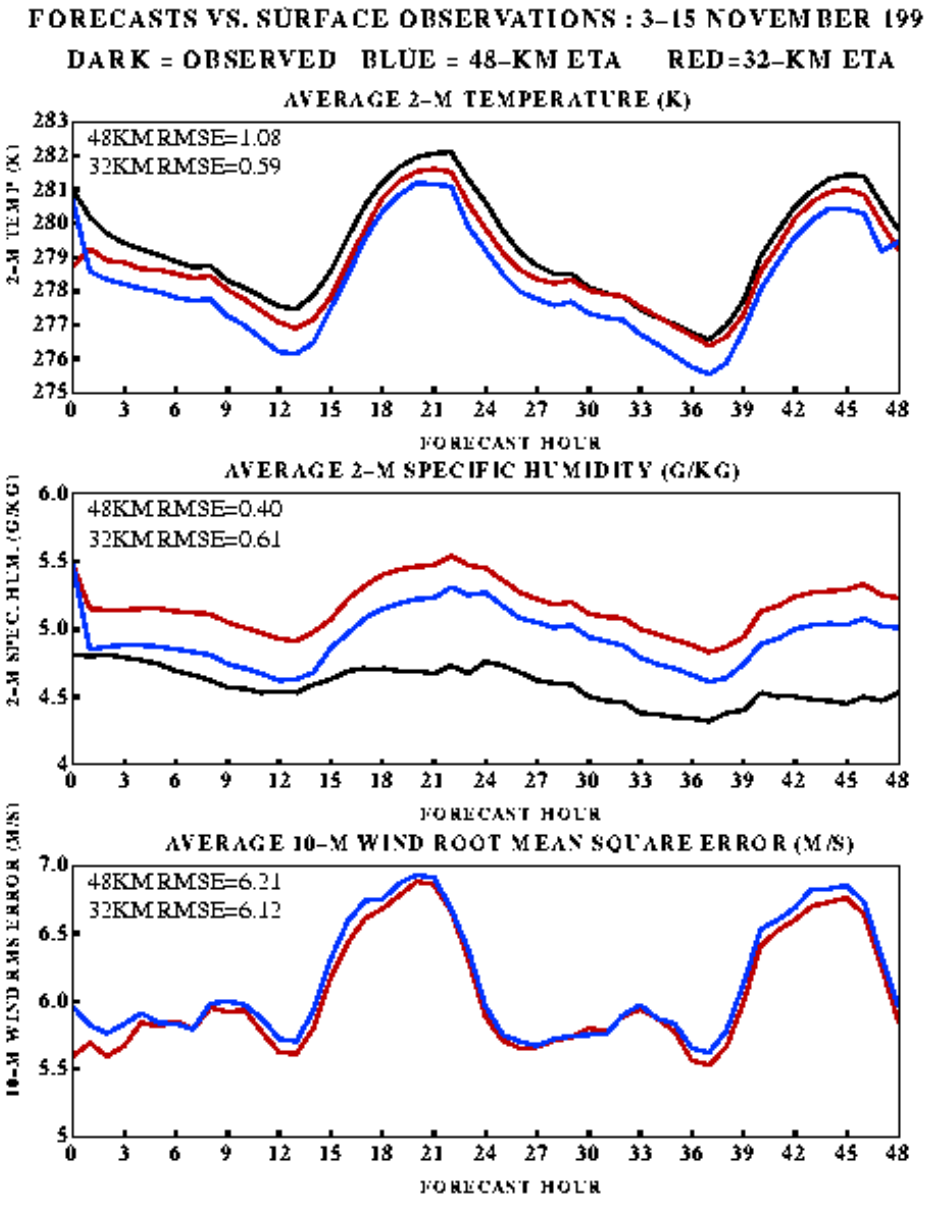

Figure 10 : (Top) Average of 2–m temperature (deg K) for 0–48 h forecast at the location of Eta model station output from the Eta–48 (blue), the Eta–32 (red), and surface observations (dark). Average RMS error for all forecast hours is printed at the upper left. (Middle) Same as top, but for 2–m specific humidity. (Bottom) Same as top, but for 10–m vector RMS error.

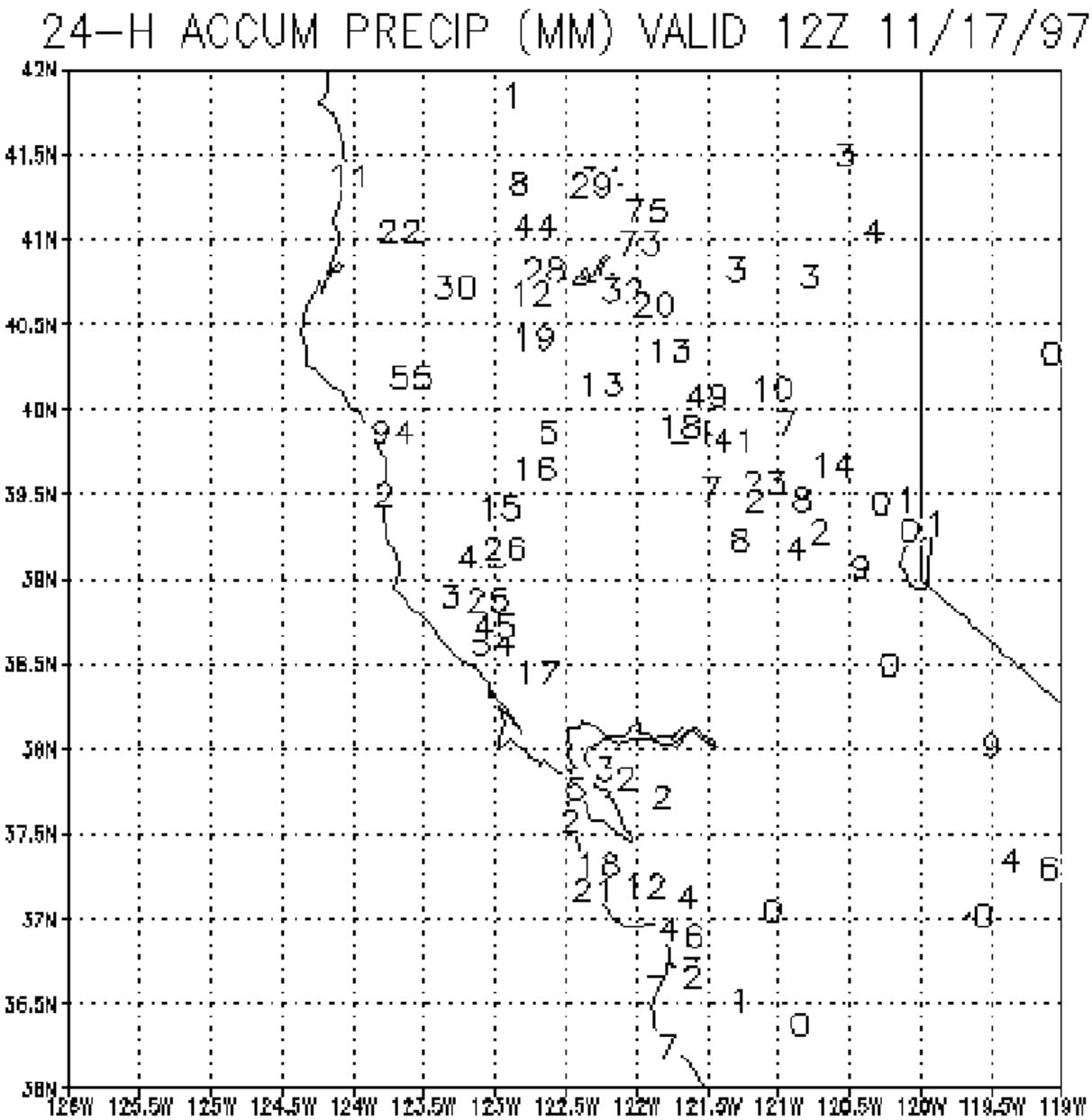
24-H ACCUM PRECIP (MM) VALID 12Z 11/17/97
42N
41.5N
41N
40.5N
40N
39.5N
39N
38.5N
38N
37.5N
37N
36.5N
36N
126W 125.5W 125W 124.5W 124W 123.5W 123W 122.5W 122W 121.5W 121W 120.5W 120W 119.5W 119W

Figure 11

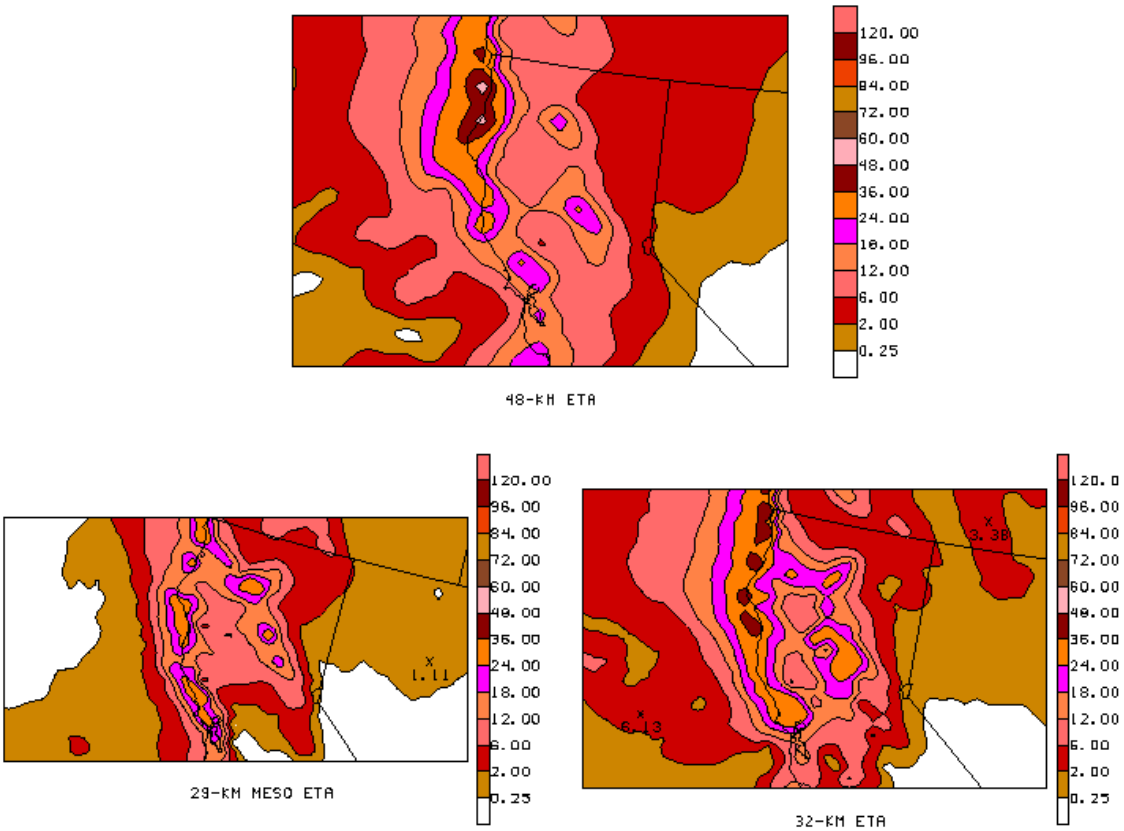

Figure 12. 0-24 h forecast of accumulated precipitation from the Eta-48 (top), the Eta-29 (bottom left) and the Eta-32 (bottom right) valid at 1200 UTC 17 November 1997. Coutours in mm: 0.25, 2, 6, 12, 18, 24, 36, 48, 60, 72, 84, 96, 120.

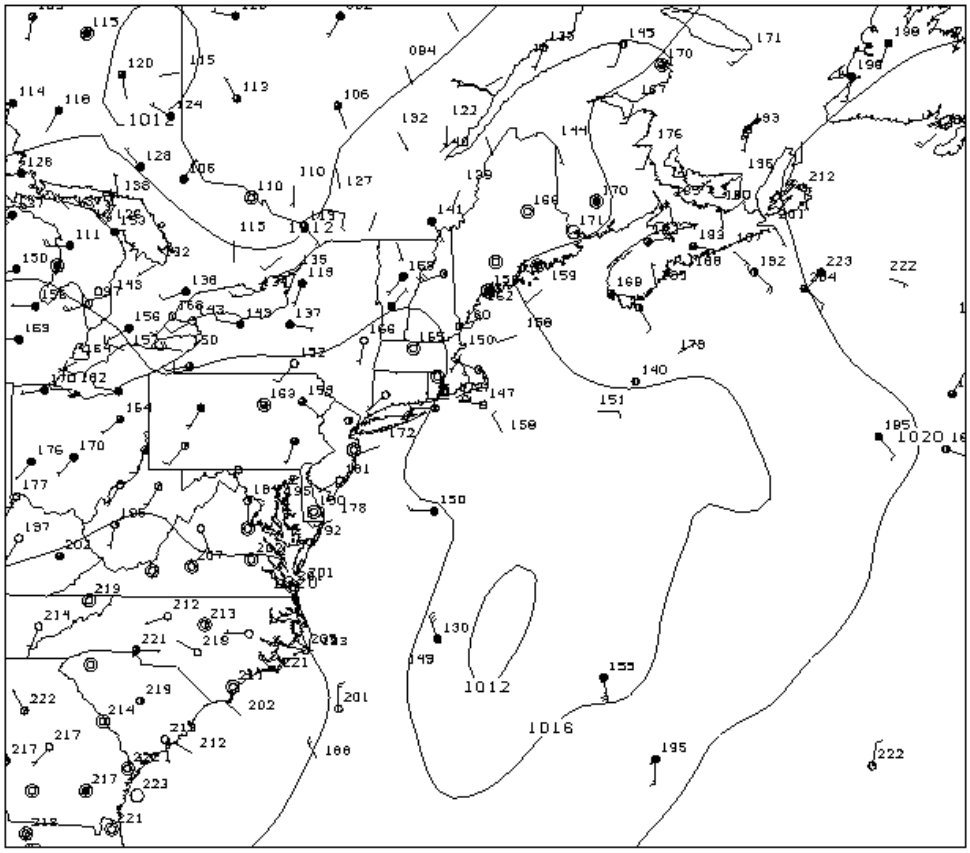

FIGURE 13 : GDAS ANALYSIS MEAN SLP VALID 00Z 11/20/97
November 1997 surface wind (kt) and sea level pressure observations. Contour interval = 4 mb.

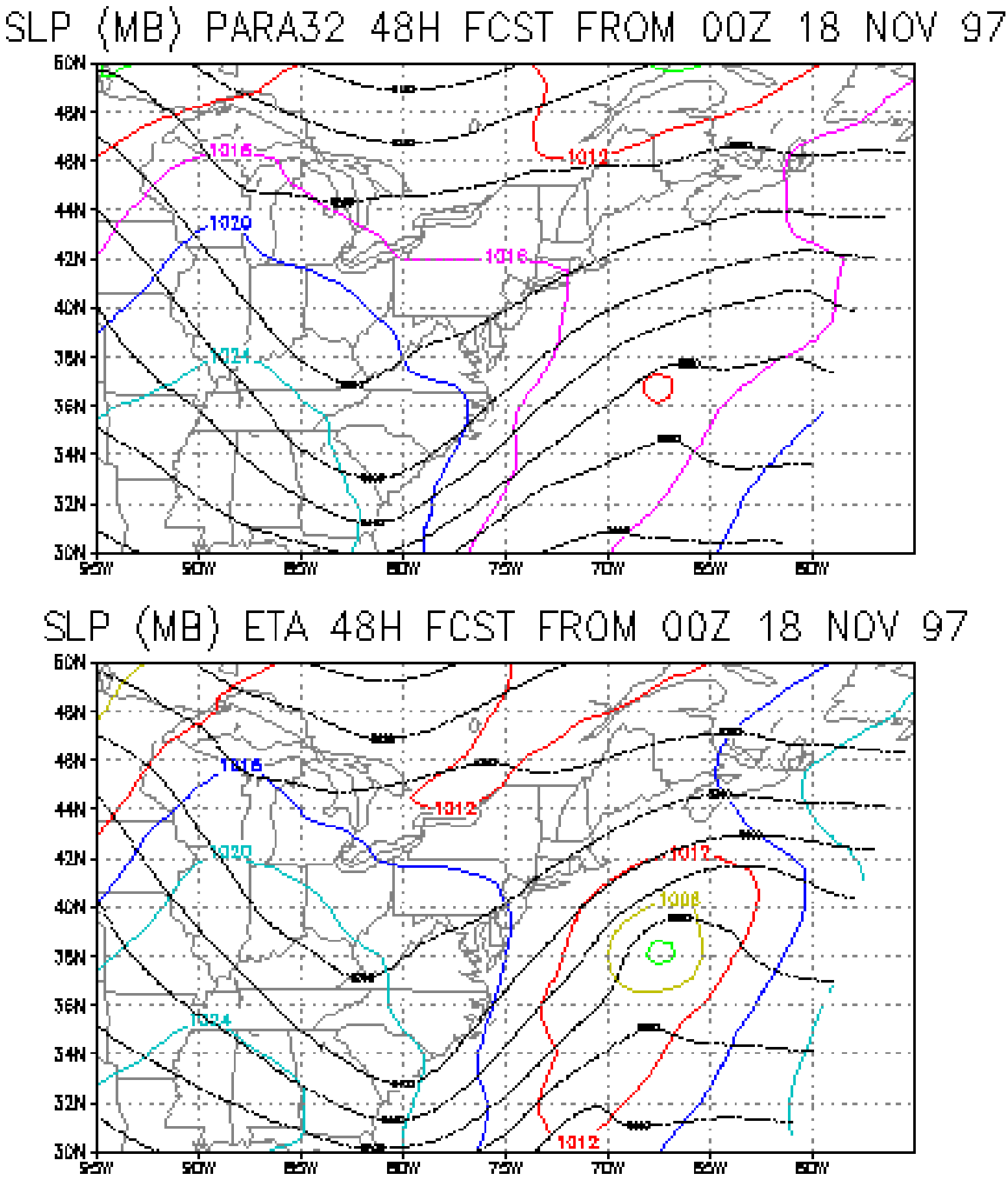

Figure 14. Eta-48 (ETA, bottom) and Eta-32 (PARA32, top) 48-h forecasts of mean sea level pressure (mb) / 1000-500 mb thickness (dam) valid at 0000 UTC 20 November 1997.

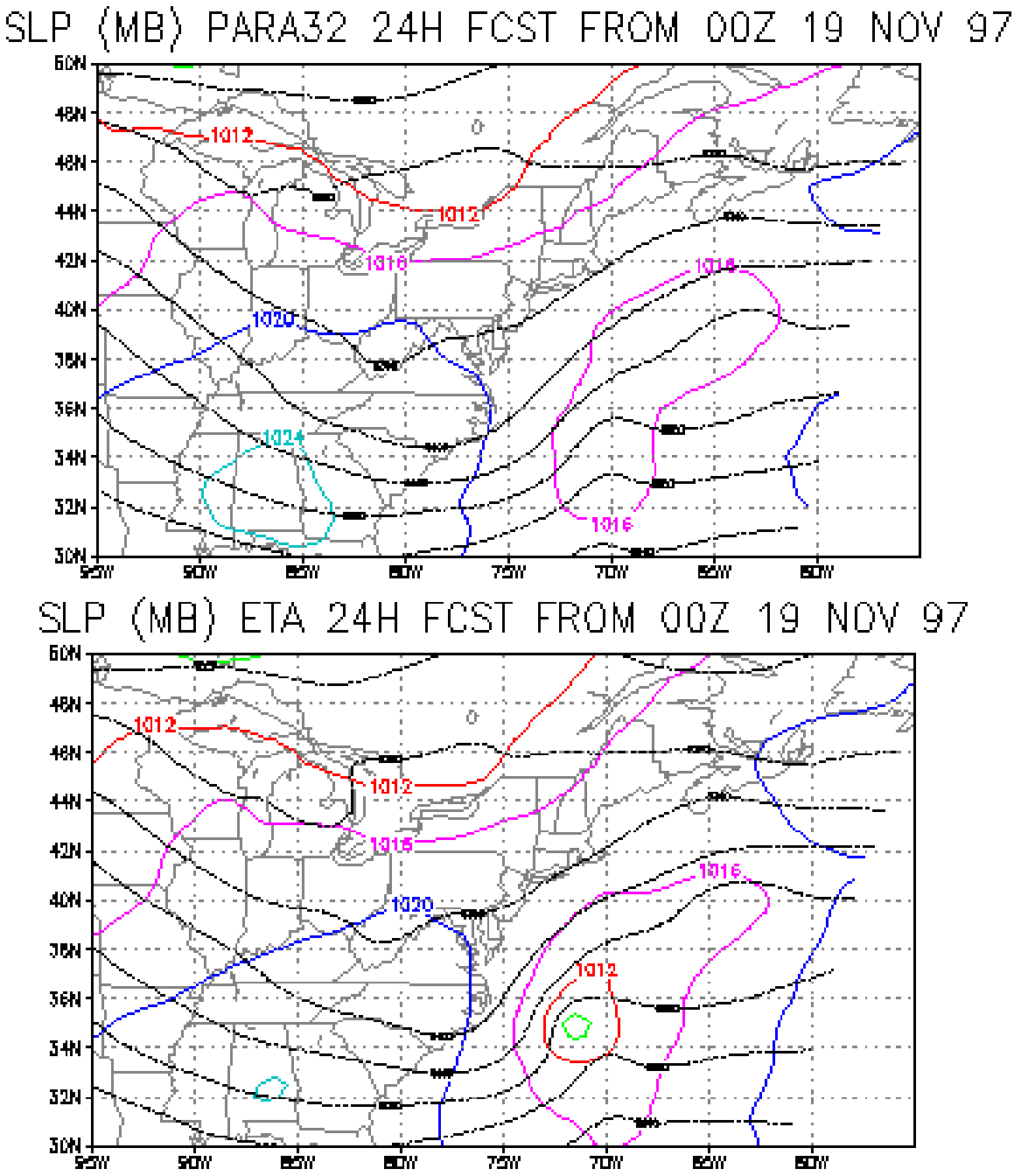

Figure 15. Same as Figure 14 but for 24-h forecasts from the Eta-48 (bottom) and the Eta-32 (top) valid at 0000 UTC 20 November 1997